Effect of Sea Ice on the Salinity of Antarctic Bottom Waters

J. R. TOGGWEILER AND B. SAMUELS

Geophysical Fluid Dynamics Laboratory/NOAA, Princeton, New Jersey

(Manuscript received 27 December 1993, in final form 6 December 1994)

ABSTRACT

Brine rejection during the formation of Antarctic sea ice is known to enhance the salinity of dense shelf waters in the Weddell and Ross Seas. As these shelf waters flow off the shelves and descend to the bottom, they entrain ambient deep water to create new bottom water. It is not uncommon for ocean modelers to modify salinity boundary conditions around Antarctica in an attempt to include a "sea ice effect" in their models. However, the degree to which Antarctic salinities are enhanced is usually not quantified or defended.

In this paper, studies of shelf hydrography and $\delta^{18}O$ are reviewed to assess the level of salinity enhancement appropriate for ocean general circulation models. The relevant quantities are 1) the salinity difference between the water masses modified on the shelves and the final offshelf flow and 2) the flux of salt (or freshwater) that gives rise to this salinity difference. Onshelf/offshelf salinity changes in the Weddell and Ross Seas appear to be fairly small, 0.15–0.20 salinity units. The quantity of brine needed to produce this salinification is equivalent to the salt drained from $\leq$0.50 m of new sea ice every year.

Salt fluxes and salinity distributions from three GCM simulations are then compared. The first model has its surface salinities simply restored to the Levitus observations. Levitus restoring produces a slight freshening in the area of the Weddell and Ross Sea shelves. The global-mean bottom-water salinity in this model is 34.57 psu, which is 0.16 units less than observed. The second model includes a very modest salinity enhancement in the area of the Weddell and Ross Sea shelves. This produces a salt flux equivalent to the formation of ~0.50 m yr^{-1} of new sea ice. Even though this amount of salt input is close to the amount observed, global-average deep salinities in the second model are only 0.02 units greater than the deep salinities in the first model. The third model includes a large salinity enrichment, which is applied throughout the Weddell and Ross embayments without regard to water depth. Its deep salinities are 0.18 units higher than the deep salinities in the first model, but the amount of salt pumped into the model greatly exceeds the salt flux in nature.

The authors conclude that salt from sea ice is probably not a major influence on the salinity of Antarctic bottom waters. Predicted salinities in ocean GCMs are too fresh because of circulation deficiencies, not because of inadequate boundary conditions. Models that employ large salinity modifications near Antarctica run the risk of grossly distorting the processes of deep-water formation.

1. Introduction

It is widely believed that brine rejection during the formation of Antarctic sea ice contributes significantly to the salinity and density of Antarctic bottom waters. Oceanographers think this is true for two reasons. First, cold, saline water is observed atop the continental shelves in the Weddell and Ross Seas (Brennecke 1921; Mosby 1934; Deacon 1937). The salinity of the densest shelf water (~34.8) is higher than the salinity of any surrounding water mass (Jacobs et al. 1979), so it is clear that brine rejection has played a role in the formation of dense shelf water. Remnants of the cold, saline shelf water have been observed descending to the sea floor along the continental slope (Foster and Carmack 1976). New bottom water is clearly derived from the water masses observed on the slope (Foldvik et al. 1985; Gordon et al. 1993).

Corresponding author address: Dr. J. R. Toggweiler, Geophysical Fluid Dynamics Laboratory, NOAA, P.O. Box 308, Princeton, NJ 08542.

A second piece of evidence comes from the distribution of $\delta^{18}O$ in seawater. The $^{18}O/^{16}O$ ratio in seawater is altered by evaporation and precipitation much like salinity. But it is only weakly altered when sea ice forms. Craig and Gordon (1965) observed that newly formed Antarctic bottom water is nearly one salinity unit saltier than offshelf Antarctic surface waters with the same $\delta^{18}O$ content. Broecker (1986) interpreted the $\delta^{18}O$, salinity offset between surface waters and newly formed bottom water as a 0.9 unit salinity enrichment due to brine rejection.

We will attempt to show that the evidence for a strong Antarctic sea ice effect has been misinterpreted. Shelf waters become colder and saltier during a slow (~5 year) generally westward traverse across the shelves (Gill 1973; Foldvik et al. 1985; Jacobs et al. 1985), but the actual salinity enrichment appears to be rather small. The modified shelf water sinking along the Weddell and Ross Sea continental slopes appears to be only 0.15–0.20 salinity units saltier than the mixture of water masses from which it originated. This level of salinification is nowhere near the 0.9 unit increase suggested by Broecker's (1986) interpretation of the $\delta^{18}O$ data. Antarctic bottom waters are relatively salty, not because of sea ice, but because the water flowing onto the Weddell and Ross Sea shelves contains a large component of salty Circumpolar Deep Water (CDW).

Our object in writing this paper is twofold. First, we would like to show how the $\delta^{18}O$, salinity relationship can be reinterpreted to fit a scenario in which the effect of brine enrichment is quite small. Second, we would like to show how the idea of a strong Antarctic sea ice effect has misled ocean modelers. Ocean general circulation models (GCMs) run in a fully prognostic mode have a tendency to generate Antarctic bottom waters that are too fresh. Because the sea ice effect is perceived to be so strong, there is a natural temptation to enhance salinities around Antarctica in a way that "simulates the effect of brine rejection." We find that the sea ice effect in nature is too small to have much effect on large-scale salinity distributions.

2. Water and salt budgets for the Weddell and Ross Sea continental shelves

The Weddell and Ross Seas are large embayments on the perimeter of the Antarctic continent. Both seas contain continental shelves that are unusually deep, about 500 m below the surface at their seaward edges. The water covering each continental shelf is itself partly covered by massive glacial ice shelves, which extend northward from the southern end of each embayment. At the seaward end of each continental shelf there is a region about 100–400 km wide that is mostly covered by sea ice. Strong southeasterly winds blow the sea ice offshore during austral winter, opening up an area near the ice-shelf front where extensive cooling and sea ice freezing can take place.

Warren (1981) describes the oceanographic setting in which sea ice formation in the Weddell Sea contributes to the formation of bottom water. In the following passage Warren refers extensively to the work of Gill (1973).

> Although near-surface water in the open Weddell Sea has a temperature close to the freezing point, it is generally too fresh to be dense enough to sink through the water below. On the shelf, however, the salinity can be increased by salt release during ice formation, and there more saline water is, in fact, found, which is dense enough to sink to depth. By itself the annual cycle of freezing and melting at the sea surface cannot account for the greater salinity of the water on the shelf, because whatever salt were added to the water during winter freezing would be mixed back into the melt water during summer. Nor can it be supposed that the salt-enriched water formed during winter immediately leaves the shelf, because it is found during summer both on the shelf and flowing down the continental slope. . . . Evidently there is a prevailing offshore movement of the pack ice that transports potential melt water locked up in ice out of the region, thus allowing a net brine production. A plausibly estimated value for the net effective rate of ice formation on the continental shelf, through the seasonal cycle, is about $1\ \mathrm{m \cdot yr^{-1}}$.

Gill (1973) inferred a slow east to west transport on the Weddell shelf itself, wherein the salinity increases along the direction of flow due to brine rejection. Gill estimated that the total offshelf flow to be about 2×10^6 $\mathrm{m^3\ s^{-1}}$. This level of flow yields a shelf residence time of about 5 years.

The most direct assessment of a sea ice effect is the change in salinity between onshelf and offshelf flows. The onshelf flow is composed of two main water types, the relatively warm, salty deep water, which circles the Antarctic continent at depths of 300–1500 m, and the so-called winter water (WW), which lies just above the deep water off the shelves (Foster and Carmack 1976; Foldvik et al. 1985; Jacobs et al. 1985; Gordon et al., 1993). The deep water in the Ross Sea is known as Circumpolar Deep Water (CDW), while the Weddell variety is a colder, fresher derivative of CDW, called Warm Deep Water (WDW). The warm, salty character of CDW (0.0°–1.5°C, 34.64–34.72 psu) is maintained by a continuous input of salty deep water from the North Atlantic. Winter Water (−1.8°C, 34.30–34.50 psu), or sometimes temperature minimum water, is formed locally by winter freezing. It remains too fresh with respect to the underlying deep water to sink below a few hundred meters. A mixture of deep water and WW is found at depths of 300–500 m along the shelf break in both the Weddell and Ross Seas.

Shelf waters in the eastern parts of the Weddell and Ross Sea embayments, where the onshelf flow begins, tend toward the composition of WW. These water masses are called eastern shelf water (ESW) in the Weddell and low-salinity shelf water (LSSW) in the Ross Sea. Warmer and saltier mixtures of deep water and winter water are observed intruding onto the shelves in the central and western portions of the embayments. These mixtures are called modified warm deep water (MWDW) in the Weddell Sea and warm core water (WMCO) in the Ross Sea. Figure 1 shows cross-shelf sections of temperature and salinity from the midshelf region of the Ross Sea (Jacobs et al. 1985). A clear intrusion of WMCO water (−0.9°C, 34.54 psu) onto the shelf is captured in this section.

In the western part of the Weddell and Ross Sea shelves one finds the saltiest and densest shelf water types, western shelf water (WSW) in the Weddell, and high-salinity shelf water (HSSW) in the Ross (see Fig. 1). WSW and HSSW (−1.8° to −1.9°C, 34.70–34.85 psu) are clearly derived from winter cooling and freezing of surface waters on the shelf. Some WSW in the Weddell Sea is observed to flow under the ice shelf and to reemerge as a supercooled and fresher water mass known as Ice Shelf water, or ISW (−2.2°C, 34.64 psu: Foldvik et al. 1985; Schlosser et al. 1990). ISW is

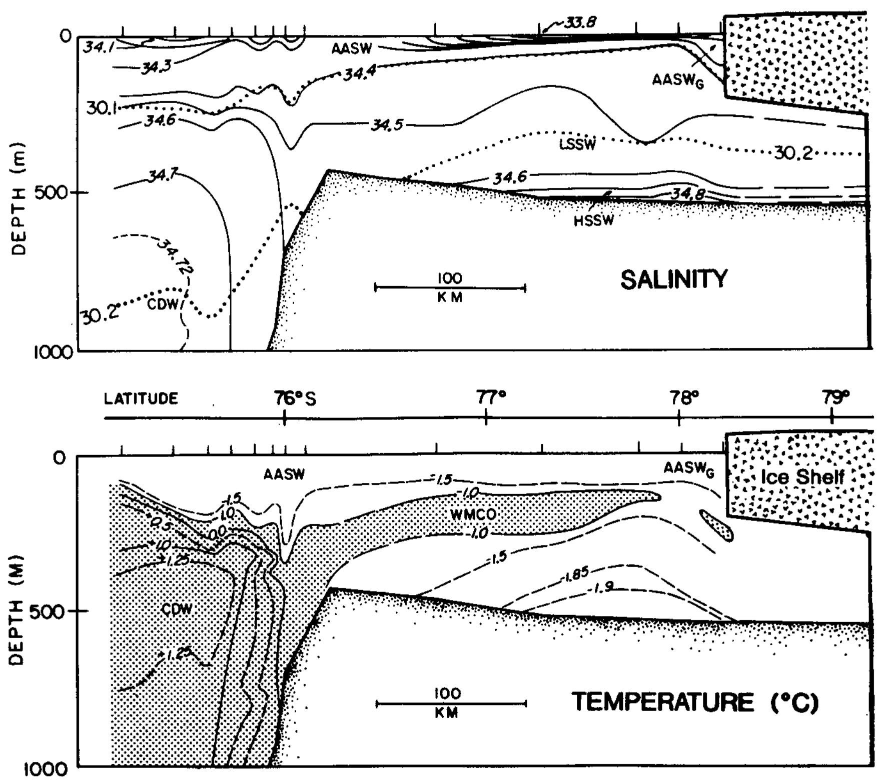

FIG. 1. Salinity (top) and temperature (bottom) across the Ross Sea continental shelf at approximately 171°W longitude. Water mass WMCO (warm core) is an intrusion of Circumpolar Deep Water (CDW) onto the shelf. Brine-enriched high salinity shelf water (HSSW) sits just above the shelf bottom. [Reproduced from Jacobs et al. (1985)].

fresher than WSW because it contains a small amount of melted glacier ice. It is colder than the surface freezing point because it comes into contact with the melting glaciers at depths of 200–400 m where the in situ freezing point is depressed by the ambient pressure.

WSW and HSSW are never observed to flow off the shelves in their pure states. They seem to remain ponded on the shelf bottom for relatively long periods of time and leave the shelf only after mixing with other water masses (Foster and Carmack 1976; Jacobs et al. 1985). Ice Shelf water in the Weddell, on the other hand, is observed nearly in its pure state at the seaward end of the Filchner Depression (Foldvik et al. 1985). Foldvik et al. find water very similar to ISW on the continental slope between 1000 and 2000 m. The offshelf and downslope movement of ISW may be aided by a thermobaric effect that comes into play because ISW is so exceptionally cold (Killworth 1977).

Figure 2 shows a *T–S* diagram for the Weddell shelf reproduced from Foldvik et al. (1985). With the exception of a thin layer of freshwater near the surface, Weddell shelf salinities lie in a range between the freshest ESW (~34.30) and the saltiest WSW (~34.80). If the onshelf flow consisted entirely of ESW with a salinity of 34.30 psu and the entire offshelf flow consisted of WSW with a salinity of 34.80 psu, then the salinity enrichment due to sea ice formation would be 0.50 units. The actual salinity enrichment is much smaller than 0.50 units because these salinity extrema are not representative of the average onshelf and offshelf flows. As stated above, the onshelf flow is a mixture of WDW and WW/ESW, with an average salinity that is probably close to that of MWDW in Fig. 2, 34.45–34.50 psu. The average offshelf flow is probably best characterized by the salinity of ISW (34.65). This leaves a net salinification of roughly 0.15–0.20 units.

A larger net salinity enrichment can be called for only if a large quantity of fresh surface water (33.8–34.3) advects onto the shelves and is subsequently converted into a saltier offshelf flow. It is hard to know for certain how much surface waters contribute; none of the cited discussions of shelf hydrography identify surface water as a major contributor to the onshelf flow. Jacobs et al. (1985) show that the fresh surface waters of the Ross Sea shelf can be locally produced from a mixture of deeper shelf water and sea ice meltwater.

While a net salinification of the offshelf flow does not seem to be very large, the brine from sea ice plays an important role in countering freshwater inputs on the shelves. The primary inputs of fresh water to the shelves are from precipitation and melting glacier ice. Using temperature and salinity alone, one cannot dis-

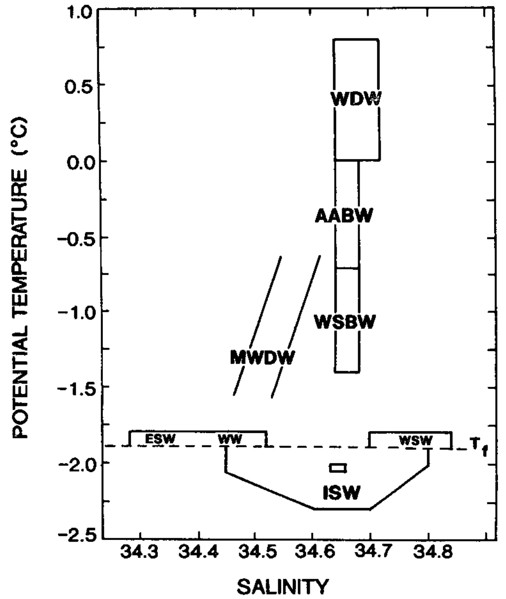

FIG. 2. T–S diagram illustrating the relationships between water masses on the Weddell Sea continental shelf (after Foldvik et al. 1985). Water mass abbreviations are explained in the text. T_f is the surface freezing point.

tinguish these freshening effects from sea ice–induced salinification. The Jacobs et al. (1985) study of the Ross Sea shelf includes a large number of $\delta^{18}O$ measurements that separate these two effects. The removal of freshwater into sea ice leaves the water behind enriched in salt, but it has a very small effect on the $^{18}O/^{16}O$ ratio of either the ice or the water. Precipitation and meltwater, on the other hand, are depleted in $\delta^{18}O$ to varying degrees.

Figure 3 summarizes a freshwater budget constructed by Jacobs et al. (1985) for the Ross shelf. Three sources of freshwater—local precipitation, glacial meltwater, and the onshelf advection of low-salinity water—balance the formation and offshelf advection of roughly 1 m yr^{-1} of sea ice. Jacobs et al. first assume a small input of freshwater from local precipitation, 0.15 m yr^{-1}. According to Jacobs et al., the water flowing onto the Ross Sea shelf is a mixture of offshelf surface water (34.1), WW (34.3), and CDW (34.7). Jacobs et al. assume that the mixture is dominated by CDW such that the average salinity for the onshelf flow is 34.46. Jacobs et al. determine that the average offshelf flow has a salinity of 34.59 psu. This leaves a net salinity enrichment for the Ross Sea shelf of 0.13 units.

Salinity enrichment can be used to determine a salt input to the shelf if the residence time of water on the shelf is known. Similarly, the meltwater/shelf water $\delta^{18}O$ difference can be used to determine the amount of glacial meltwater that is added to the shelf. Jacobs et al. suggest a shelf residence time of 6 years. This implies an onshelf/offshelf flow of about 1.3 Sv (Sv $\equiv 10^6$ m^3 s^{-1}). A 1.3 Sv input of 34.46 water, coupled to the loss of 34.59 psu water, is equivalent to a fresh water addition of 0.33 m yr^{-1} over the shelf. A 6-year residence time and the observed $\delta^{18}O$ depletion require 0.36 m yr^{-1} of glacial meltwater. These additions, plus 0.15 m yr^{-1} of precipitation, define a total freshwater input of 0.84 m yr^{-1}. To maintain balance, 0.84 m of freshwater must be advected away in the form of ice, while its salt is left behind. Because sea ice has a residual salinity of ~4 psu, a slightly greater thickness of sea ice is required, 0.95 m yr^{-1} in this example.

According to Jacobs et al. (1985), the offshelf advection of ~1 m yr^{-1} of sea ice is consistent with a representative shelf residence time and observed levels of onshelf/offshelf salinity enrichment and $\delta^{18}O$ depletion. Shorter shelf residence times require larger meltwater inputs and larger amounts of sea ice formation. Most importantly, the study of Jacobs et al. (1985) shows that more than half the brine added to shelf waters goes into negating the effect of freshwater additions on the shelf. The brine input, which actually makes the offshelf flow saltier, is equivalent to the formation and removal of $\leqslant$0.50 m yr^{-1} of sea ice. As will be discussed below, this is a flux that can be directly compared with the surface fluxes generated by GCM boundary conditions.

In summary, sea ice brine makes certain shelf waters (e.g., WSW and HSSW) as much as 0.50

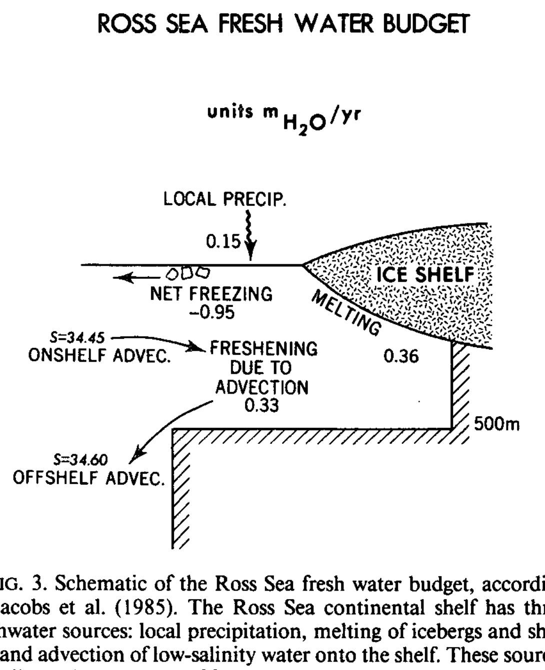

FIG. 3. Schematic of the Ross Sea fresh water budget, according to Jacobs et al. (1985). The Ross Sea continental shelf has three freshwater sources: local precipitation, melting of icebergs and shelf ice, and advection of low-salinity water onto the shelf. These sources contribute about 0.84 m of fresh water to the shelf every year. These inputs are balanced by the offshelf advection of 0.95 m of new sea ice with a residual salt content of 4 ppt. Jacobs et al. determine the onshelf advection of fresh water (0.33 m yr^{-1}) by dividing the offshelf/onshelf salinity difference (0.134) by the average salinity (34.5), multiplying by the average shelf depth (500 m), and dividing by the shelf residence time, ~6 yr.

units saltier than the water flowing onto the shelves. But other shelf processes, mainly the melting of fresh water from the ice shelves, make shelf waters fresher. By all measures, the net salinification of the water leaving the Antarctic shelves appears to be rather small, 0.15–0.20 units. Brine input that counteracts additions of freshwater contributes to the formation of bottom water by preventing shelf waters from becoming too fresh, but it does not make the offshelf flow saltier.

Brine production is known to enhance the salinity of WW in the open ocean regime off the shelves, but this enrichment does not lead to the production of bottom water. Martinson (1990) has shown that the vertical structure characteristic of the open ocean regime, that is, cold, fresh surface water overlying warm salty deep water, is stabilized by the warm temperatures of the underlying deep water. If sea ice formation makes the winter surface water salty enough to initiate convection into the deep water, the warm water brought up from below immediately melts the new sea ice. The melting restores fresh water to the surface layer, restores the pycnocline, and shuts down the convection. Martinson's regulatory mechanism explains why the vertical water column beyond the shelves is close to being unstable in winter but cannot easily cross over into a condition of wholesale deep convection.

3. The $\delta^{18}O$–salinity relationship

Jacobs et al. (1985) used $\delta^{18}O$ measurements on the Ross Sea shelf to construct a freshwater budget consistent with a small onshelf/offshelf salinity enrichment. As cited in the introduction, Craig and Gordon (1965) and Broecker (1986) used $\delta^{18}O$ information to infer a very large salinity enrichment in the Weddell Sea. In this section we would like to illustrate how such radically different interpretations can be drawn from the same tracer.

When water evaporates from the ocean it leaves the seawater left behind saltier and more enriched in ^{18}O. When water vapor condenses and falls back into the ocean, the receiving water becomes fresher and more depleted in ^{18}O. Thus, $\delta^{18}O$ levels in ocean surface water vary linearly with salinity over most of the ocean. Craig and Gordon (1965) noted that the deep waters of the World Ocean, particularly the bottom waters of the Weddell Sea, fall off this trend. Figure 4 shows the global trend in the GEOSECS $\delta^{18}O$ data as it was graphed by Broecker (1986). Weddell Sea Bottom Water (WSBW) is 0.9 salinity units saltier than surface waters with the same $\delta^{18}O$. Indian and Pacific deep waters are ~0.6 salinity units saltier than surface waters with the same $\delta^{18}O$.

The basic problem with the interpretations of Craig and Gordon (1965) and Broecker (1986) stems from

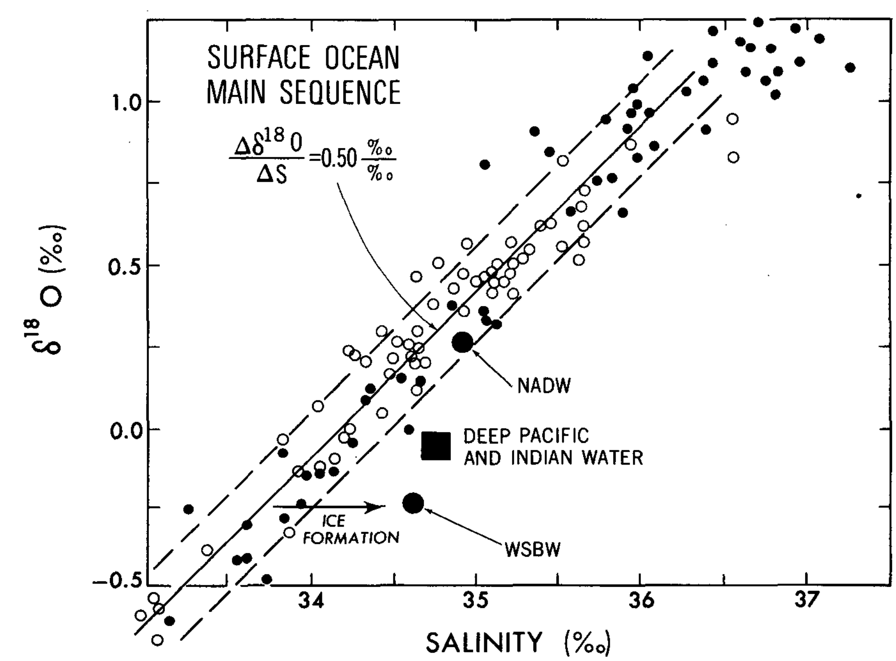

FIG. 4. Plot of $\delta^{18}O$ vs salinity showing major ocean water masses, according to Broecker (1986). Surface waters over the entire globe plot along a single trend, which can be extrapolated to an $\delta^{18}O$ value of −17‰ at zero salinity. This suggests that evaporation and precipitation fractionate oxygen isotopes by nearly constant amounts. Deep waters of the world ocean, especially Weddell Sea Bottom Water (WSBW), fall off the trend. Broecker suggests that sea ice formation in the Weddell Sea has increased the salinity of WSBW by 0.9 ppt without changing the $\delta^{18}O$.

the fact that these authors did not consider any $\delta^{18}O$ information from the Antarctic shelves: shelf observations were not available to Craig and Gordon in 1965; Broecker's analysis in 1986 was limited to open ocean GEOSECS $\delta^{18}O$ observations. Weiss et al. (1979) published $\delta^{18}O$ observations from a small number of Weddell shelf water samples collected during the International Weddell Sea Oceanographic Expedition (IWSOE 73). Weiss et al. (1979) were the first to demonstrate the effect of glacial meltwater on shelf hydrography.

Figure 5 shows the Weiss et al. $\delta^{18}O$ results plotted in the same $\delta^{18}O$ versus salinity format as Broecker's Fig. 4. The $\delta^{18}O$, S composition of WSBW is the same in both Broecker's and Weiss et al.'s diagrams. The Weiss et al. WDW overlies the $\delta^{18}O$, S composition of Broecker's Indian and Pacific Deep Water. Weiss et al. showed that Ice Shelf water and WSW in the Weddell Sea are much more depleted in $\delta^{18}O$ than WSBW (-0.66 and -0.47 per mil, respectively, vs -0.29 per mil). No surface water anywhere in the Antarctic is depleted enough to account for the $\delta^{18}O$ in ISW and WSW. The only possible source for this very low $\delta^{18}O$ water is the meltwater from the Antarctic ice sheet itself. The ice in the Antarctic ice sheet, and consequently the ice in the Weddell ice shelves, is extremely depleted in $\delta^{18}O$ (as low as -55 per mil) due to the progressive distillation of $H_2{}^{18}O$ from the snow that falls on top of the ice sheet. A small amount of glacial meltwater added to $-0.3‰$ shelf water is capable of dramatically lowering the $\delta^{18}O$ of shelf water (Schlosser et al. 1992).

Comparison of the $\delta^{18}O$, salinity plot in Fig. 5 with the T–S plot in Fig. 2 illustrates the ability of $\delta^{18}O$ to differentiate shelf water masses. Cooling of surface water can lower water temperatures only to the freezing point. Thus ESW, WW, and WSW in Fig. 2 all have the same temperature. ISW is slightly cooler due to its formation at depth below the ice shelf. The input of a tiny amount of meltwater, on the other hand, can differentiate these water masses more strongly if certain ones get more meltwater than others. One sees in Fig. 5 that the addition of meltwater pulls the $\delta^{18}O$ of Ice Shelf water and western shelf water well below the $\delta^{18}O$ of warm deep water and winter water. Ice Shelf water contributes directly to new Weddell Sea Bottom Water; thus the meltwater in ISW pulls down the $\delta^{18}O$ of WSBW (Schlosser et al. 1992). WSBW has the same $\delta^{18}O$ as winter water even though it is 1° warmer.

Glacial meltwater seems to act as a "point source" of extremely depleted $\delta^{18}O$ that depresses the $\delta^{18}O$ of WSBW and AABW. When introduced in small quantities, the point source can label new bottom water without also making it too fresh. Antarctic Bottom Water flows into all of the ocean basins and eventually cycles back to the circumpolar region (Broecker et al. 1985). Thus deep water in the Indian and Pacific feels the affect of the point source as does Circumpolar Deep Water itself. It is possible that ~75% of the ocean's deep waters might be feeling the effect of glacier ice on the Weddell shelf.

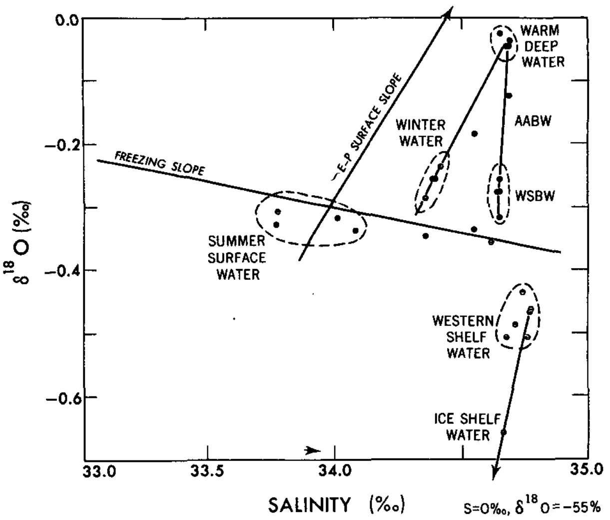

FIG. 5. Relationship of $\delta^{18}O$ vs salinity for water masses in the Weddell Sea (after Weiss et al. 1979). The arrow labeled "E-P surface slope" corresponds to the lower end of Broecker's "Surface Ocean Main Sequence" (Fig. 4). Weiss et al. argue that the $\delta^{18}O$-depleted western shelf water and Ice Shelf water acquire their low $\delta^{18}O$ contents from melting shelf ice with a $\delta^{18}O$ of $-55‰$ and zero salinity.

$\delta^{18}O$, the hydrological cycle, and the underlying circulation

Craig and Gordon (1965) and Broecker (1986) explain the $\delta^{18}O$, S anomaly in the Weddell Sea as the effect of a massive salt source large enough to affect the whole ocean. Following the work of Weiss et al. (1979) and Jacobs et al. (1985), we interpret the $\delta^{18}O$, S anomaly as the effect of a point source of glacial meltwater. These interpretations lend themselves to very different views of the hydrological cycle and the underlying circulation. Broecker (1986) constructs a box model for the cycling of ^{18}O in the ocean and atmosphere that illustrates his point of view. We have illustrated Broecker's model in the context of a water mass evolution diagram in the top panel of Fig. 6.

Broecker sees the formation of AABW in terms of a thermohaline circulation in which ~15 Sv of midlatitude surface water flows poleward and becomes transformed through surface freezing into new bottom water in the Weddell Sea. During its poleward flow, roughly 1 Sv of freshwater must be added to the midlatitude surface water in order to reduce its salinity from ~36 to 33.8. In order for bottom water to form, enough salt must be added to raise the salinity of Antarctic surface waters by 0.9 units back up to 34.7 psu. This requires a tremendous amount of sea ice formation.

The alternative view is expressed in the bottom panel of Fig. 6. Implicit in this point of view is that the surface

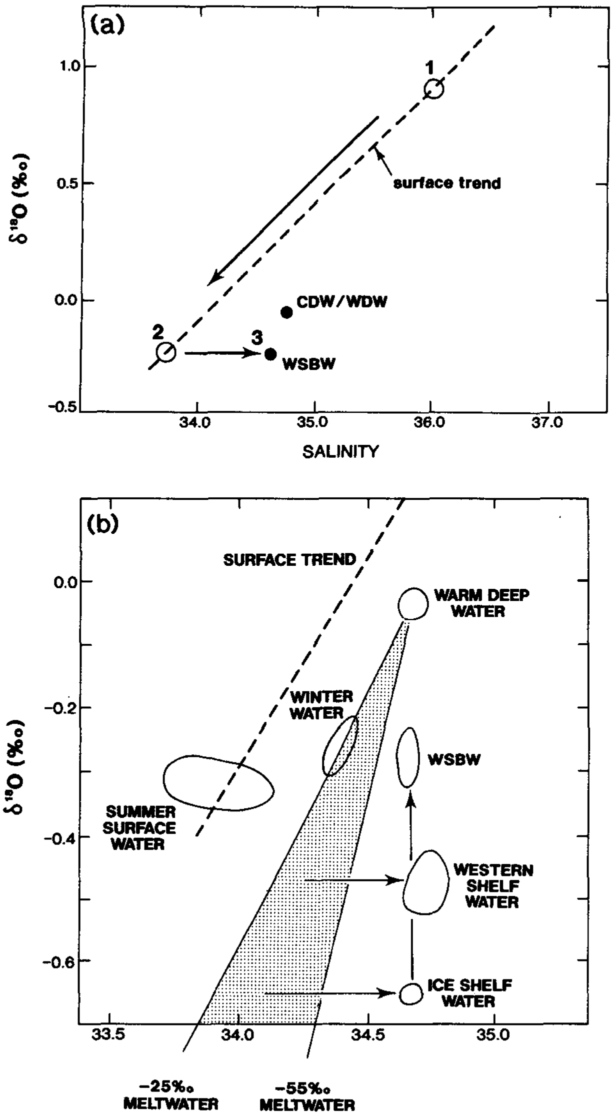

FIG. 6. Schematic showing two different views of the $\delta^{18}O$–salinity relationship. In the top panel, high-latitude precipitation makes mid-latitude surface water 1) ($S = 36.0$) fresher and lighter in $\delta^{18}O$ as it flows poleward to become Antarctic surface water. A huge amount of brine must be added to Antarctic surface water 2) ($S = 33.8$) to raise its salinity 0.9 salinity units to the level of Weddell Sea Bottom Water 3) ($S = 34.66$). In the bottom panel, bottom water production is initiated from a mixture of warm deep water and two glacial meltwater types. One (−55‰) characterizes ice formed in the center of the continent; the other (−25‰) characterizes ice formed near the edge of the continent. Brine is added to the WDW/meltwater mixture to form western shelf water and Ice Shelf Water. These water masses mix with warm deep water as they flow off the shelf and descend down the continental slope to form WSBW. The salt enrichment in new WSBW, which can be attributed to sea ice brine, is the salinity difference between the WDW/meltwater mixture and WSBW, about 0.2 salinity units.

waters in the Southern Ocean flow equatorward as part of the Ekman drift under the circumpolar westerlies. In this view, the precipitation, which lowers the salinity and $\delta^{18}O$ of Antarctic surface waters in the open ocean, flows northward away from the shelves and plays no role in the formation of bottom water. The poleward flow that is eventually converted into new bottom water comes mainly from Circumpolar Deep Water. The $\delta^{18}O$ evolution of shelfwaters is thereby dominated by contributions from WDW/CDW and glacial meltwater (Jacobs et al. 1985).

In the bottom panel of Fig. 6, we modify Weiss et al.'s (1979) $\delta^{18}O$, S diagram (Fig. 5) to show warm deep water mixing with a range of glacial meltwater types. At one end of the range is a meltwater with a $\delta^{18}O$ of −25 per mil, a value which might characterize the ice melting from the north face of the ice shelf (Jacobs et al. 1985). Winter water in this diagram lies on a mixing line connecting −25 per mil meltwater and warm deep water. Jacobs et al. note that Ross Sea surface waters collected within 10 km of the ice shelf and Ross Sea winter water (TMIN in their nomenclature) have $\delta^{18}O$, S compositions that are too low in $\delta^{18}O$ to have formed by freezing of typical surface water. These low $\delta^{18}O$ levels point to an input of meltwater from the nearby ice sheet. At the other end of the meltwater range is a meltwater with a $\delta^{18}O$ of −55 per mil, an extreme value which characterizes the ice formed in the center of the continent (Weiss et al. 1979). Glacier ice sampled at the bottom of a bore hole through the Ross Ice shelf has a $\delta^{18}O$ in the middle of this range of −40 to −43 per mil (Grootes and Stuiver 1983).

As drawn in the bottom panel of Fig. 6, brine rejection displaces WDW/meltwater mixtures toward the compositions of Ice Shelf water and western shelf water. The net displacement of ISW and WSW from the center of the WDW/meltwater shaded area is about 0.60 salinity units. ISW and WSW mix with WDW as they flow off the shelf and down the slope. The final product, WSBW, is about 0.20 units saltier than a simple mixture of WDW and glacial meltwater. This level of salinification is very close to the salinity increases between onshelf and offshelf flows in the Weddell and Ross Seas as noted above.

In Broecker's scenario, surface waters in the Antarctic move poleward, collecting precipitation over the whole Southern Ocean. Brine formation on the shelves must partially negate the effect of all this precipitation. However, Antarctic surface waters do not generally move poleward. They drift primarily toward the north and carry most of the precipitation falling on the Southern Ocean out of the region. Under this scenario, the brine from sea ice negates only freshwater additions on or near the shelves. The freshwater added to the shelves includes the precipitation on the Antarctic ice sheet, which is slowly released to the shelves as glacial meltwater.

4. How a model sees the effect of sea ice formation

The Ross Sea freshwater budget in Jacobs et al. (1985) makes a critical distinction. Jacobs et al. estimate that more than half of the brine production on the Ross Sea shelf negates local inputs of fresh water. This is important from the point of view of an ocean model that does not directly include the effects of glacial meltwater or precipitation.

A model's boundary conditions should be expected to simulate the net transfer of salt (or fresh water) into or out of the ocean. Thus, brine production that negates *local* sources of fresh water is not seen by a model as a net flux of salt. Only the brine production in excess of the local freshwater input should be considered as part of a model's boundary conditions. If the results of Jacobs et al. can be extended to include the Weddell Sea and other shelf areas around Antarctica, the salt flux that needs to be duplicated in GCMs amounts to the salt drained from some 33 cm of new ice per year. This is the amount of sea ice formation needed to raise the salinity of the onshelf flow by ~0.15 salinity units. It is not a very large input of salt.

Most ocean GCMs simulate the effect of freshwater fluxes across the air–sea interface by restoring surface salinities toward observed values. The restoring operation is parameterized in a model's salinity equation by a term, $\gamma_s(S^* - S)$, where S^* is the observed salinity in a model grid box, S the predicted salinity, and γ_s an inverse time constant applied to salinity. If brine production is active on a shelf, and is reflected in a high S^*, an onshelf flow of fresher water will cause γ_s $(S^* - S)$ on the shelf to be positive. A positive salt flux counteracts the onshelf flow of fresher water and helps maintain shelf salinities close to their observed values.

Multiplying $\gamma_s(S^* - S)$ by the depth of the surface layer (Δz) and dividing by 35 (the average salt content of seawater in g kg^{-1}) produces an implied freshwater flux, which is directed in the opposite direction from the salt flux but has the same effect on salinity. The implied water flux has units meters per year. This is the way model salt fluxes are usually diagnosed. In a region containing sea ice, the diagnosed water flux includes the effect of an increase or decrease in ice thickness. If the diagnosed water flux in the area of the Ross Sea shelf is close to +0.33 m yr^{-1} (positive in this case indicating a freshwater flux out of the ocean), the model has duplicated the net ice growth determined in the Jacobs et al. (1985) water budget.

The problem with the salinity restoring method in regions of sea ice formation is that observed near-surface salinities do not reflect the process of brine enrichment. Basically, the average salinities used in constructing the Levitus dataset do not reflect conditions and times of year when sea ice is actually formed and subsurface shelf waters are mixed up to the surface. Average near-surface salinities (upper 50 m) in the highest latitudes of the Weddell and Ross Seas are about 34.4–34.5 psu (Levitus 1982). If a model restores its Weddell and Ross Sea salinities to the observed upper-50-m salinities (34.4–34.5), it will not be able to make new bottom water with a salinity of 34.66 psu.

Modelers often modify salinity boundary conditions around Antarctica so that the boundary conditions incorporate some kind of extra salinification. This is usually done by increasing S^*. Bryan and Lewis (1979) increased S^* in the highest latitudes of the Weddell and Ross Seas to 35.0 psu while using a restoring time constant of $1/30$ d^{-1}. Cox (1989) increased S^* to 35.4 psu but used a weaker time constant, $1/400$ d^{-1}. The "Antarctic Salt" model in Toggweiler and Samuels (1993) restores surface salinities to 35.0 psu in the two grid rows closest to Antarctica (73°S and 78°S) using a time constant of $1/120$ d^{-1}. England (1992, 1993) increases S^* to 34.9 psu in his southernmost row of grid points (78°S) using a time constant of $1/50$ d^{-1}. England tapers his modified S^* back toward the observed values such that all S^* south of 69°S are modified. None of these studies gives the salt fluxes or implied water fluxes that are produced by these modifications.

5. A model study of the sea ice effect

We have run out several different coarse-resolution models in which the values of S^* in the Weddell and Ross Sea embayments are systematically altered. The object is to monitor the implied water fluxes in order to compare the computed values with the 0.33 m yr^{-1} net sea ice effect estimated by Jacobs et al. (1985) for the Ross Sea continental shelf. The model used in these examples is the 4.5° lat × 3.75° long × 12 level model described by Toggweiler et al. (1989a,b; hereafter TDB89) and Toggweiler and Samuels (1993). It is forced by annual mean boundary conditions at the surface. Wind stresses are taken from Hellerman and Rosenstein (1983). Predicted temperatures and salinities in the model's first layer (Δz = 51 m) are restored to Levitus (1982) temperatures and salinities averaged over the upper 50 m. Each example is run out 2 000 years to an equilibrium state.

Observations like those in Fig. 2 show quite clearly that the dense water ponded on Antarctic shelf bottoms contains sea ice brine. One can use this information to construct a simple boundary condition that incorporates a sea ice effect. In an experiment we will call "500-m restore," we replace surface S^* in the shelf areas of the Weddell and Ross Seas with the 500-m salinities in the Levitus dataset; that is, we restore surface salinities to the values found at 500 m just above the shelf bottom. The new S^* derived in this way are typically about 0.4 psu higher than S^* derived from data in the upper 50 m.

In a second experiment called "Antarctic Salt," surface S^* are replaced with salinity values of 35.0 in the two highest latitude grid rows of the model. No attempt is made to limit the region of elevated S^* by bottom depth. The modified salinity restoring in Antarctic Salt

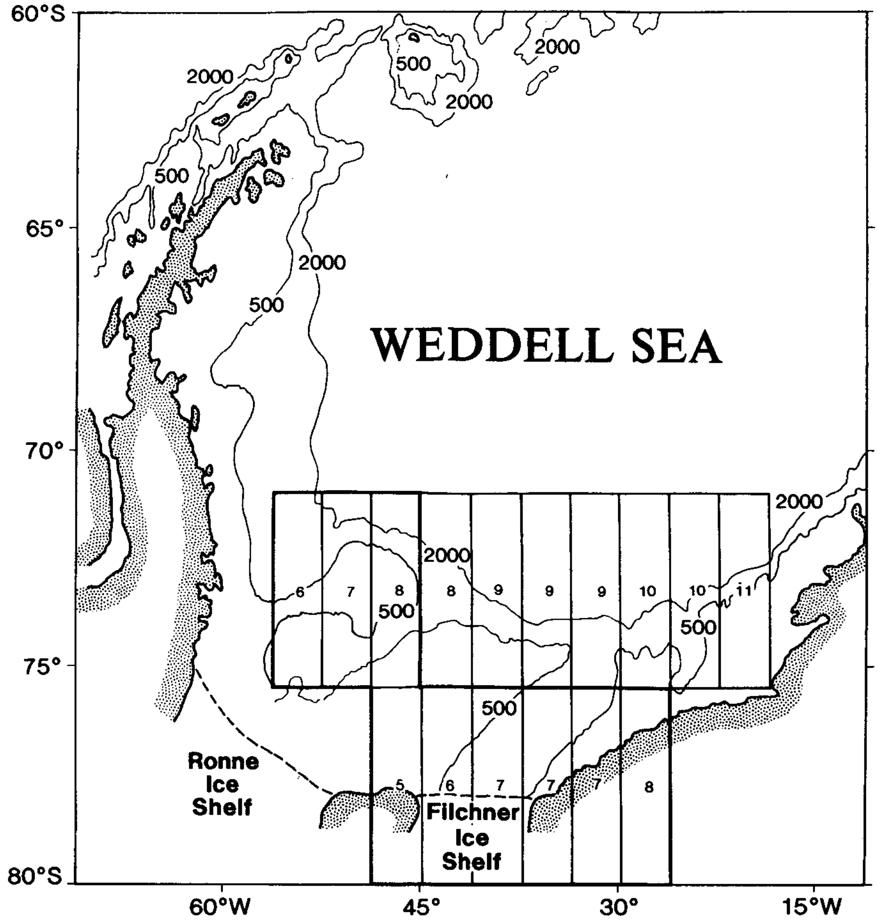

FIG. 7. Bathymetry of the Weddell Sea with overlaid model grid showing the location of model grid boxes within the Weddell embayment. Bold outline on the model grid highlights the area where the actual bathymetry defines a shelf. Numbers in the grid refer to the deepest model level at that location, bottom depths as follows: 5 = 595 m, 6 = 914 m, 7 = 1347 m, 8 = 1898 m, 9 = 2559 m, 10 = 3311 m, 11 = 4131 m, and 12 = 5000 m.

experiment mimics the level and geographic extent of the restoring in Bryan and Lewis (1979), Cox (1989), and England (1992, 1993). Results of the Antarctic Salt experiment were presented originally in Toggweiler and Samuels (1993).

A particular problem with the Antarctic Salt approach is the depth of the water column where S^* is modified. Adding salt to water sitting on a shelf is very different from adding salt to surface waters that overlie deep water. A low level of brine rejection added to the slow-moving water on a shelf can gradually build up shelf salinities to their observed levels. Enhanced S^* in areas far away from the continent, or in a model without resolved shelves, can immediately induce convection to great depth. This grossly distorts the actual situation. As reviewed above, sea ice–induced convection in the deep-water regime is self-limiting because the warm deep water raised from below quickly melts the sea ice (Martinson 1990). A model that simulates the sea ice effect with enhanced S^* is not regulated in this way. It can continue to convect without limit. It will pump huge quantities of salt into the deep water and can potentially pump huge quantities of heat into the atmosphere.

Figure 7 shows a map of the Weddell Sea along with the 500-m and 2000-m isobaths. Overlaid on the map are the outlines of model grid boxes in the two model grid rows that lie within the Weddell embayment. Figure 9 shows a similar reconstruction for the Ross Sea. The bottom depth in each model grid box is given by a number that refers to the deepest model level at each grid location (for exact depths, see caption to Fig. 7). Given the coarseness of the grid and the smoothing employed in constructing the model bathymetry, the continental shelves in these embayments are only weakly resolved.

In Figs. 8 and 10 a series of four panels gives the Antarctic S^* used in four different model runs. Each panel shows the Weddell or Ross Sea grid configuration with the appropriate S^* enclosed in each box. The top

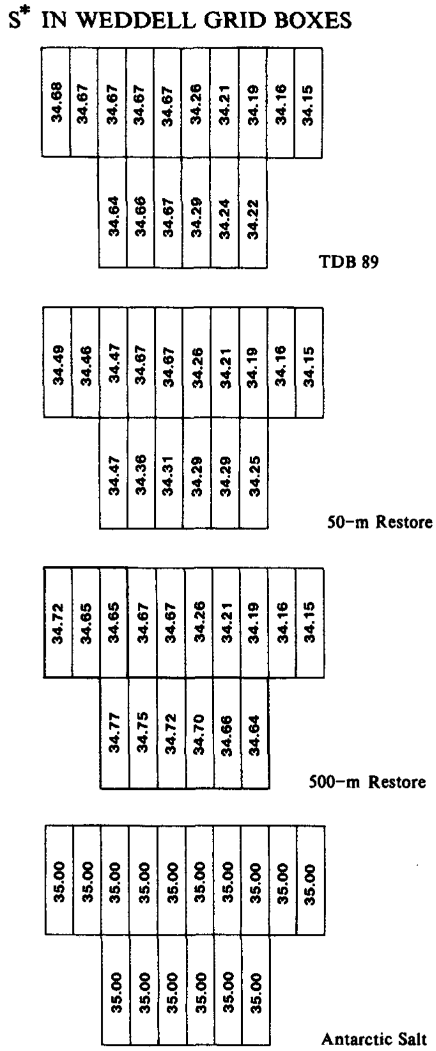

FIG. 8. S^* used to force model salinities in the Weddell sector. Salinity values are shown within the model grid configuration illustrated in Fig. 4. The four panels show S^* in Toggweiler et al. (1989a,b), 50-m restore, 500-m restore, and Antarctic Salt. For the 500-m restore experiment S^* are modified only where the actual bathymetry defines a shelf. Shelf grid boxes are highlighted by the bold outline.

panel gives the S^* used by TDB89. For the reasons given below, this field of S^* is not used in this paper. The second panel shows the actual 50-m salinities as interpolated from the Levitus (1982) dataset. This set of S^* forms the boundary conditions for a control case, which we will call "50-m restore". The third panel shows the 500-m salinities in the grid boxes where the actual topography says there should be a shelf. "Shelf" grid boxes are delineated within a bold outline in Figs. 7–10. The S^* in the third panel are used in 500-m restore. The fourth panel is filled with S^* of 35.0 psu over both grid rows. These are the S^* used in Antarctic Salt. The restoring coefficient for salinity, γ_s, is set to $1/120\ d^{-1}$ in each experiment. (TDB89 used a restoring coefficient of $1/30\ d^{-1}$.)

TDB89 reported that the S^* used in their study were derived from an average of the upper 50-m salinities in Levitus (1982). We found, however, when we looked in detail, that the S^* in the western corners of the Weddell and Ross Seas did not correspond very well to the Levitus salinities. Figures 7 and 9 show that there are significant areas in the Weddell and Ross embayments where the model has ocean, but the real bathymetry has land. The original mapping procedure used by TDB89 to "fill" these areas produced an S^* field that did not adequately represent the low salinities observed along the coast. A more appropriate fill procedure was used to generate the S^* field for the 50-m restore experiment. The S^* in the western corners of the Weddell and Ross Seas are about 0.2 psu lower in 50-m restore than they were in TDB89. Given the weak $1/120\ d^{-1}$ restoring parameter used in these experiments, the difference between the S^* field in TDB89 and that of 50-m restore is ultimately not very important.

Table 1 summarizes the water fluxes in 50-m restore, 500-m restore, and Antarctic Salt. Water fluxes are zonally averaged in each grid row and in each embayment and are then combined into a single mean value covering both grid rows and both embayments. Water fluxes in 50-m restore are slightly negative in both latitude bands in both the Weddell and Ross Seas. Water moving onto the shelves is slightly saltier than the 34.25–34.50 psu Levitus S^*. When the model attempts to restore its surface salinities toward the fresher S^*, it removes salt from the surface layer and produces an effective water flux into the ocean.

Water fluxes in 500-m restore are generally positive (i.e., model salinities increase) in both embayments. Mean water fluxes in the southernmost latitude band (77.8°S) are 0.64 m yr^{-1} in the Weddell Sea and 0.48 m yr^{-1} in the Ross Sea. These are 50%–100% higher than the 0.33 m yr^{-1} net flux estimated by Jacobs et al. The mean water flux in the 73.4°S latitude band, which mostly overlies deep water, is essentially zero.

The Antarctic Salt model generates net water fluxes in its southernmost latitude band that exceed those in 500-m restore by an additional 50%. It generates even larger water fluxes in the 73.4° latitude band (1.43 m yr^{-1} in the Weddell sector and 1.07 m yr^{-1} in the Ross sector) where fluxes in 500-m restore are very small. Overall, the mean water flux in Antarctic Salt exceeds the water flux in 500-m restore by a factor of 7, 1.05 versus 0.15 m yr^{-1}.

The area represented by the 77.8° grid boxes in the model is $0.70 \times 10^{12}\ m^2$ ($0.26 \times 10^{12}\ m^2$ in the Weddell and $0.44 \times 10^{12}\ m^2$ in the Ross). This is about 70% of the area actually covered by continental shelf in the Weddell and Ross embayments, excluding the shelf area covered by the ice shelves. The total shelf area around the whole perimeter of Antarctica is about 2.5 times larger than the shelf area in the Weddell and

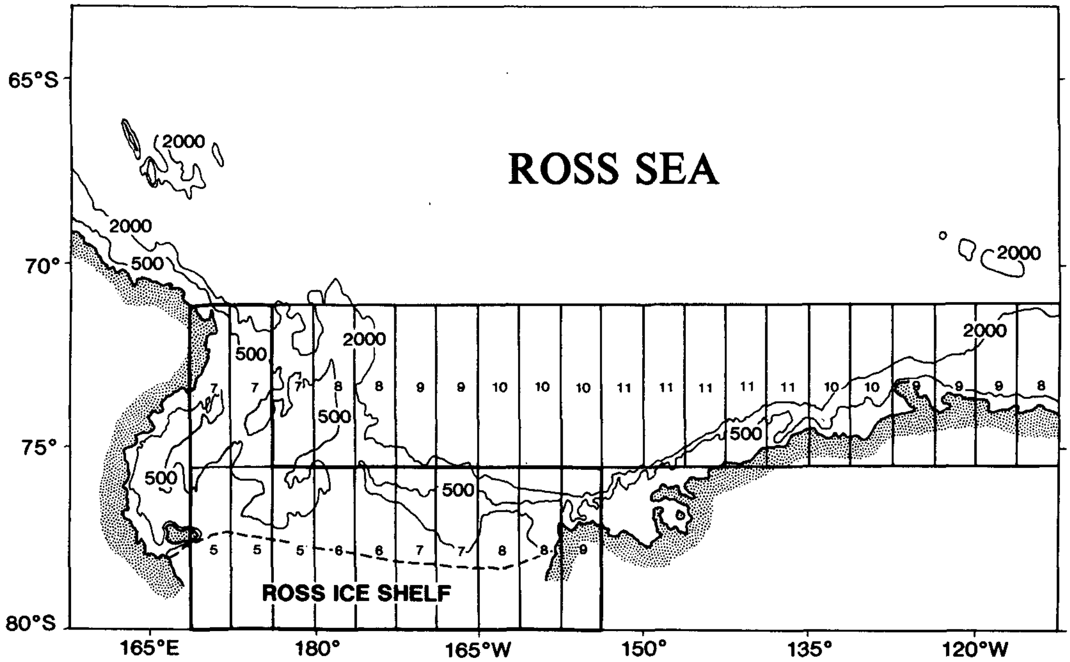

FIG. 9. Bathymetry of the Ross Sea with overlaid model grid showing the location of model grid boxes within the Ross Sea embayment. Bold outline on the model grid highlights the area where the actual bathymetry defines a shelf. Numbers within the grid refer to the deepest model level at that location (see caption to Fig. 4 for depths).

Ross embayments alone. If the Jacobs et al. water fluxes are representative of the whole Antarctic shelf, the areally integrated water flux associated with sea ice formation on the Antarctic shelves would be about twice the areally integrated flux generated by the 500-m restore model.

Figure 11 shows a comparison of global meridional streamfunctions for the 500-m restore and Antarctic Salt models. The Antarctic Salt model generates a very strong local overturning cell adjacent to Antarctica ($\sim$24 Sv). The overturning cell extends into the deepest levels of the model. The 500-m restore model generates a fairly weak overturning cell ($\sim$5 Sv). It is quite clear that the enhanced S^* in regions of deep water is leading to wholesale convection, which drives the enhanced overturning in Antarctic Salt.

Figures 12 and 13 graphically illustrate some of the differences between 500-m restore and Antarctic Salt. Figure 12 shows the predicted salinities in each model's first layer. Predicted surface salinities in 500-m restore reach about 34.60 psu, remaining 0.15–0.20 salinity units fresher than the S^* used to force the model. Predicted surface salinities in Antarctic Salt reach 34.80 psu. Figure 13 maps the implied freshwater flux (units m yr^{-1}). Implied freshwater fluxes in 500-m restore are 0.5–1.0 m yr^{-1} out of the ocean in the western half of the embayment but are mostly negative in the eastern half. Implied water fluxes in Antarctic Salt are positive everywhere and exceed +1.0 m yr^{-1} throughout the long eastern sector where the water column is deep.

Table 2 shows a comparison of global-mean salinities for each vertical layer. Mean near-bottom salinities in TDB89, 50-m restore, and 500-m restore all lie in a narrow range between 34.57 and 34.59 psu, about 0.15 salinity units fresher than observed (34.73). The difference between a slight Antarctic freshening effect, as in 50-m restore, and a moderate salinity enhancement, as in 500-m restore, amounts to only 0.02 salinity units globally. In other words, a moderate amount of salinity enhancement in the area of the Antarctic shelves increases near-bottom salinities globally by only 0.02 units. This is a fairly insignificant effect, but one which is consistent with our interpretation of the δ^{18}O, salinity data. Bottom waters in the immediate vicinity of Antarctica appear to be only 0.15–0.20 units saltier due to the production of sea ice. Mixing between newly formed bottom waters and overlying deep waters will tend to reduce the salt effect as new bottom waters flow northward. It is not unreasonable to imagine that the globally averaged salt effect may be as small as 0.05 units.

Bottom salinities in the Antarctic Salt model are close to those observed, but are 0.18 salinity units higher than those in 50-m restore. A sea ice effect of this magnitude cannot be supported. How could a sea ice effect raise the salinity of average bottom water worldwide by 0.18 units when the water flowing off the Antarctic shelves is only 0.15–0.20 units saltier?

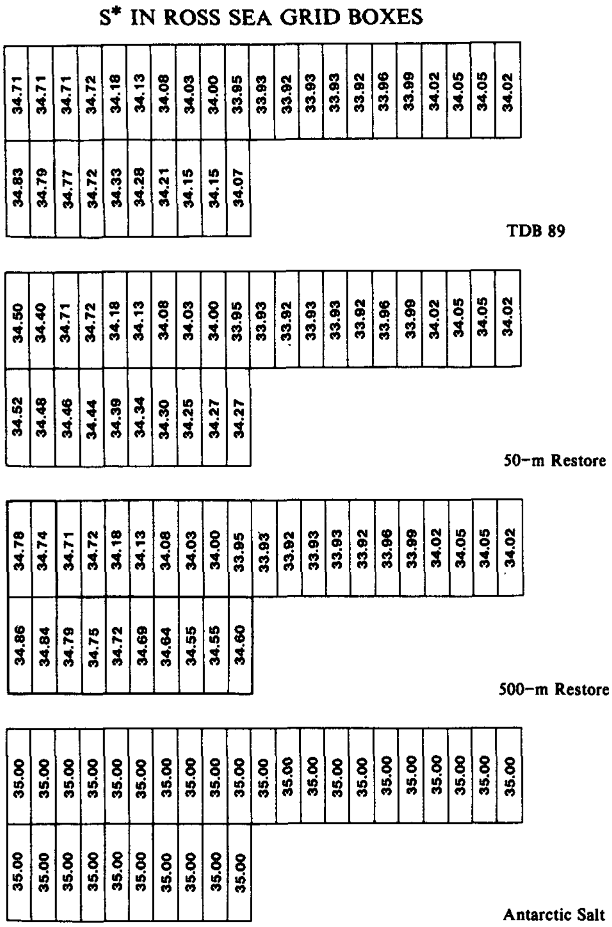

FIG. 10. The S^* used to force model salinities in the Ross sector. Salinity values are shown within the model grid configuration illustrated in Fig. 6. The four panels show S^* in Toggweiler et al. (1989a,b), 50-m restore, 500-m restore, and Antarctic Salt. For the 500-m restore experiment S^* are modified only where the actual bathymetry defines a shelf. Shelf grid boxes are highlighted by the bold outline.

6. Discussion

Salinity enhancement has been widely used by ocean modelers to bring model salinities into better agreement with observed salinities. A recent application can be found in the study of England (1993). England finds that his global model is unable to reproduce observed deep ocean salinities without some adjustment of S^* around Antarctica. He shows that stronger outflows from the Atlantic reduce the need for these adjustments but do not eliminate them entirely. From the perspective of this paper, even the "weak" S^* adjustment used in England's later experiments still produces a very substantial flux of salt.

The GCM in England (1993) has the same grid configuration and the same vertical levels as the models in this paper. The S^* in England's weak S^* adjustment are enhanced in three latitude bands, 68.9°S, 73.4°S, and 77.8°S in an attempt to simulate a sea ice effect. Here S^* is enhanced for 3 months out of 12 with a maximum S^* of 34.90 psu in the southernmost grid row. Exact values of the enhanced S^* in the 68.9° and 73.4° grid rows are not given. Model salinities are restored toward the imposed S^* field with a time constant of $1/50\ d^{-1}$. Thus, England's enhanced S^* are not as extreme as those in our Antarctic Salt model, and they are not applied year-round, but they extend one grid row further from Antarctica, and they are imposed on the model with a stiffer restoring constant.

England's weak Antarctic salinity adjustment is introduced in his Experiment X. It is removed in Experiment XI, such that any salinity differences between Experiments X and XI are due entirely to the enhanced S^* in Experiment X. These differences can be compared directly with the salinity differences between the 50-m restore and Antarctic Salt models in this paper. England's Experiments X and XI include a feature that enhances lateral mixing along isopycnal surfaces. This feature is not included in the GCM used here.

Table 3 compares the global mean salinities from our results in Table 2 with the global mean salinities from England's Experiments X and XI. Near-bottom salinities in England's Experiment X and Experiment XI are 34.66 and 34.46, a difference of 0.20 salinity units. This difference is similar to the 0.18 unit difference between 50-m restore and Antarctic Salt. It is an order of magnitude larger than the salinity difference between our 50-m restore and 500-m restore models. England's Experiment X generates a greatly enhanced

TABLE 1. Model water and heat fluxes in regions where S^* is modified.

	Implied water flux[a] ($m\ yr^{-1}$)		Implied heat flux[b] ($W\ m^{-2}$)	
Experiment	Weddell sector	Ross sector	Weddell sector	Ross sector
		50-m restore		
73.4°S	−0.005	−0.21	58	24
77.8°S	−0.065	−0.031	23	7
mean[c]	−0.12		27	
		500-m restore		
73.4°S	0.16	−0.11	57	27
77.8°S	0.64	0.48	29	28
mean[c]	0.15		33	
		Antarctic Salt		
73.4°S	1.43	1.07	76	99
77.8°S	0.98	0.67	27	24
mean[c]	1.05		71	

[a] Positive sign indicates water flux out of ocean.
[b] Positive sign indicates heat flux out of ocean.
[c] Mean of combined Weddell and Ross Sea sectors in which contributions from 73° and 78°S latitude bands are weighted by longitudinal extent.

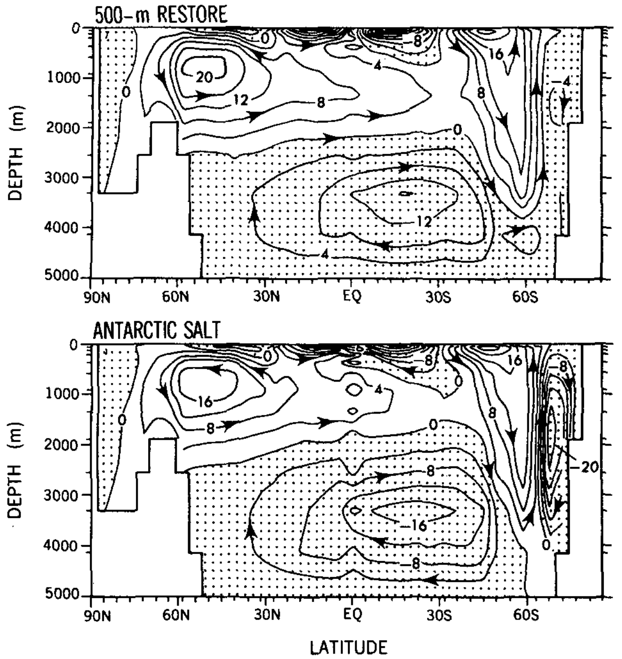

FIG. 11. Comparison of global meridional overturning from the 500-m restore (top) and Antarctic salt (bottom) models. The Antarctic Salt model generates a 24-Sv overturning cell adjacent to Antarctica in comparison with a 5-Sv overturning cell in 500-m restore. The overturning next to Antarctica in the 50-m restore model (not shown) is about 2 Sv.

overturning cell adjacent to Antarctica, which is also similar to the overturning cell in Antarctic Salt (Fig. 11). These similarities suggest that the salt fluxes produced by England's weak salinity adjustment must be roughly the same as the salt fluxes derived from the strong S^* enhancement in our Antarctic Salt model.

Deep waters in our 50-m restore model and England's Experiment XI are 0.16 and 0.26 salinity units, respectively, fresher than observed, but one cannot realistically expect brine from sea ice to bring model salinities up to the observed levels. We can only conclude that attempts to increase model salinities by enhancing S^* in model boundary conditions are actually serving to mask unidentified circulation deficiencies.

a. Lack of southward CDW penetration in GCM simulations

The main problem for ocean models seems to be their inability to maintain the observed water properties at 300–1000 m just seaward of the Antarctic continent. If a model can maintain a salty water mass like CDW up against Antarctica, it will not need much added salt to make realistic Antarctic Bottom Water.

The high salinities in Circumpolar Deep Water are attributed mainly to the outflow of salty deep water from the Atlantic Ocean. The circulation in the real ocean moves Atlantic salt down to Antarctica with a minimum amount of dilution. GCMs like those used here or by England (1993) seem to have a problem in this regard. In this section we illustrate this problem by comparing model properties around Antarctica in the 500-m restore and Antarctic Salt simulations.

Figures 14 and 15 show model current vectors representing the meridional and vertical (v, w) flow, salinity, and temperature along a north–south section that terminates in the central Ross Sea. Figure 14 shows results from 500-m restore. Figure 15 shows results from Antarctic Salt. Each section consists of an average of three model grid rows centered on 174°W. At the top of each figure is the average τ_x and the divergence of the Ekman transport along the section (identical for both models). Model current vectors for the surface (Ekman) layer are very large at this scale and are not included in either figure. Figure 16 shows the observed annual mean salinity, temperature, and oxygen levels along the same section (Levitus 1982). The data in Fig. 16 is interpolated onto a more highly resolved two-degree grid.

In 500-m restore, high-salinity (>34.60) water penetrates southward from midlatitudes to 60°S at depths between 2000 and 3000 m. Water at the southern end of the salt maximum is about 1.5°C. Thus, model properties at this position are similar to CDW but are

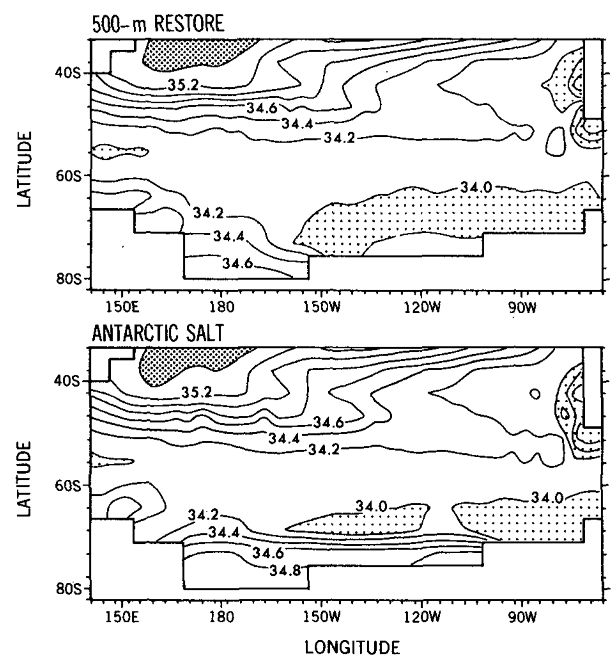

FIG. 12. Predicted salinities in the Ross Sea sector for the surface layer in the 500-m restore (top) and Antarctic Salt (bottom) models (C.I. = 0.2 psu). Figure 10 shows the salinities being restored to in both experiments. Restoring to 500-m salinities in the areas of continental shelf produces surface salinities in excess of 34.6 in the western corner of the Ross Sea (max$S$ = 34.652). Restoring to 35.0 indiscriminately over the both Ross Sea grid rows produces surface salinities in excess of 34.8 over most of the embayment (max$S$ = 34.854).

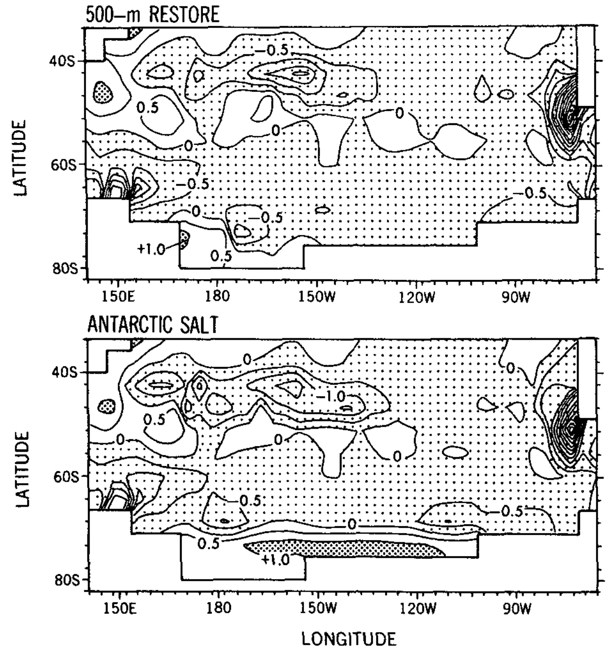

FIG. 13. Implied surface water flux (m yr^{-1}) in the Ross Sea sector in the 500-m restore (top) and Antarctic Salt (bottom) models (C.I. = 0.5 m yr^{-1}). Implied water flux out of the ocean reaches +1.0 m yr^{-1} in the western corner of Ross Sea in 500-m restore but exceeds +1.0 m yr^{-1} over most of the embayment in Antarctic Salt.

about 0.1 salinity units too fresh. The main problem with the model solution is that the model's "CDW" does not extend farther south. The model also produces a small amount of 34.60 psu water at the southern end of the section, which is clearly generated by the 500-m restore boundary conditions. A gap remains between the 34.60 psu water masses at 60°S and 78°S. The observations in Fig. 16 show that the core of CDW in the real world is characterized by a continuous salt maximum that extends from 40°S right up to the shelf region at 75°S.

The Antarctic Salt model has higher salinities overall, but its middepth salinity maximum is shallower and does not extend as far south as the salinity maximum in 500-m restore. Temperatures at the southern end of the salinity maximum are also warmer, 1.5°–2.5°C. These warm temperatures suggest that the salt maximum in Antarctic salt bears less resemblance to CDW than the salt maximum in 500-m restore. As its name suggests, the Antarctic Salt model has some very high salinity water adjacent to Antarctica. The model's high-salinity Antarctic water extends well out onto the slope to depths of 3000 m. The high-salinity water is also very cold, much of it less than −0.5°C. Observations show that water colder than −0.5°C is confined to the shelf or to the winter water up near the surface. New bottom water in Antarctic Salt is clearly spilling out of the Ross Sea to a much greater extent than is observed.

Almost coincident with the observed salinity maximum in Fig. 16 is an oxygen minimum, which extends poleward into the Ross Sea. Low oxygen levels are a well-known characteristic of CDW. In addition to its low oxygen content, CDW is also low in radiocarbon. Broecker et al. (1985) characterize CDW as a blend of middepth waters from the Atlantic, Indian, and Pacific Oceans. The observed high salinity, low oxygen, and low $\Delta^{14}C$ in CDW are not locally generated. These properties must be advected down to Antarctica. They cannot be produced by the manipulation of model boundary conditions, and they cannot be maintained in close proximity to surface boundary conditions in the presence of large amounts of mixing or convection.

The current vectors in the top panels of Figs. 14 and 15 help one understand the property distributions produced by the two models. At 63°S, the latitude of maximum divergence in the wind field, the 500-m restore model has strong upward motion. Water converges into this latitude band from both north and south, such that the convergence dominates the circulation in this sector. Antarctic Salt also has convergence at 63°S, but the convergence in this case is fed entirely by flow from the north. There is also downslope flow all along the Antarctic continental slope. The circulation in Antarctic Salt resembles the kind of thermohaline circulation implied by Broecker's (1986) interpretation of the $\delta^{18}O$ data. Fresh upper-ocean water seems to pour into the Ross Sea where its conversion into cold salty bottom water is facilitated by the artificially high S^* in the model's boundary conditions.

The high salinity of CDW in the Ross sector is associated with the eastward transport of salty deep water from the Atlantic. Something in the model's circulation either prevents this salty water from reaching Antarctica or causes the Atlantic water to be diluted with fresher water before it can reach Antarctica. The dominant v, w flow between 50° and 65°S in Figs. 14 and 15 consists of strong poleward motions in the fresh waters of the upper 1000 m, which seem to feed into downward motions below. This circulation is common to both models but is less extreme in 500-m restore. One would certainly not infer a circulation like this from the observed property distributions. The downward motions seem to cut across the nose of the salt maximum, possibly limiting its southward extent. Circulation features of this sort seem more likely to be preventing the formation of realistic bottom waters than deficiencies in salinity boundary conditions.

b. *A note about model heat fluxes*

A recent paper by Maier-Reimer et al. (1993) reports GCM results that illustrate a related problem. The Maier-Reimer et al. model generates a very large outflow of North Atlantic Deep Water, such that deep salinities in the Southern Ocean are fairly high without any apparent enhancement by Antarctic boundary

TABLE 2. Global mean salinities (psu) in four ocean models.

Level	Depth[a] (m)	Obs[b]	TDB89[c]	50-m restore	500-m restore	Antarctic Salt
1	26	34.75	34.75	34.75	34.75	34.76
2	85	34.96	34.91	34.92	34.92	34.94
3	170	35.00	34.95	34.97	34.98	34.99
4	295	34.88	34.92	34.92	34.93	34.95
5	483	34.71	34.85	34.81	34.82	34.85
6	755	34.63	34.79	34.73	34.74	34.78
7	1131	34.65	34.76	34.73	34.74	34.80
8	1622	34.72	34.75	34.75	34.76	34.84
9	2228	34.73	34.67	34.70	34.71	34.79
10	2935	34.74	34.62	34.63	34.65	34.76
11	3721	34.73	34.58	34.59	34.61	34.75
12	4565	34.73	34.57	34.57	34.59	34.75

[a] Depth at layer midpoint (m).
[b] Observed global mean salinities (Levitus 1982) interpolated to model grid.
[c] Global mean salinities in prognostic model of Toggweiler et al. (1989a,b).

conditions. However, the Maier-Reimer et al. model uses a special boundary condition for temperature that permits very large local heat fluxes in deep-water formation areas in the North Atlantic and Antarctic. As in our Antarctic Salt model, the Maier-Reimer model generates a huge amount of overturning near the Antarctic continent. Overall, some 30 Sv sinks to the bottom adjacent to Antarctica, including 10 Sv of upper-kilometer water that flows poleward across 60°S.

A very large heat loss is required to transform this upper-ocean water into bottom water. Maier-Reimer et al.'s diagnosed heat losses in the Weddell and Ross Seas average between 100 and 150 W m^{-2} over the seasonal cycle. The regions of maximum heat loss are not confined to the shelf regions but extend well offshore. Jacobs et al. (1985) determine that heat losses over the Ross Sea shelf are only 15 W m^{-2}. Gordon (1981) suggests that the average heat loss over the deep-water regime off shore may be somewhat larger, ~31 W m^{-2}. Thus, Maier-Reimer et al.'s 100–150 W m^{-2} heat fluxes appear to be as unreasonable as the salt additions in Antarctic Salt. Table 1 includes Antarctic heat fluxes derived from the 50-m restore, 500-m restore, and Antarctic Salt simulations. Heat fluxes in the 77.8°S grid row average between 20 and 30 W m^{-2}, but reach as high as 100 W m^{-2} in the 73.4°S grid row of Antarctic Salt.

The large Antarctic heat fluxes in Maier-Reimer et al. and the large salt fluxes in our Antarctic Salt model drive huge amounts of deep convection in the deep-water regime off the shelves. These are areas where the real ocean maintains a permanent pycnocline. These models forcibly convert near-surface water, with near-surface properties, into new bottom water. The water masses being modified in nature are mainly from the ocean's interior. They are cold and salty enough to

TABLE 3. Comparison with global mean salinities in England (1993).

Level	Depth[a] (m)	Obs[b]	England expt X[c]	England expt XI[d]	50-m restore
1	26	34.75	34.75	34.78	34.75
2	85	34.96	34.90	34.91	34.92
3	170	35.00	34.89	34.90	34.97
4	295	34.88	34.80	34.79	34.92
5	483	34.71	34.64	34.63	34.81
6	755	34.63	34.52	34.51	34.73
7	1131	34.65	34.47	34.44	34.73
8	1622	34.72	34.55	34.46	34.75
9	2228	34.73	34.62	34.49	34.70
10	2935	34.74	34.64	34.47	34.63
11	3721	34.73	34.65	34.47	34.59
12	4565	34.73	34.66	34.46	34.57

[a] Depth at layer midpoint (m).
[b] Observed global mean salinities (Levitus 1982) interpolated to model grid.
[c] Global mean salinities in Experiment X of England (1993).
[d] Global mean salinities in Experiment XI of England (1993).

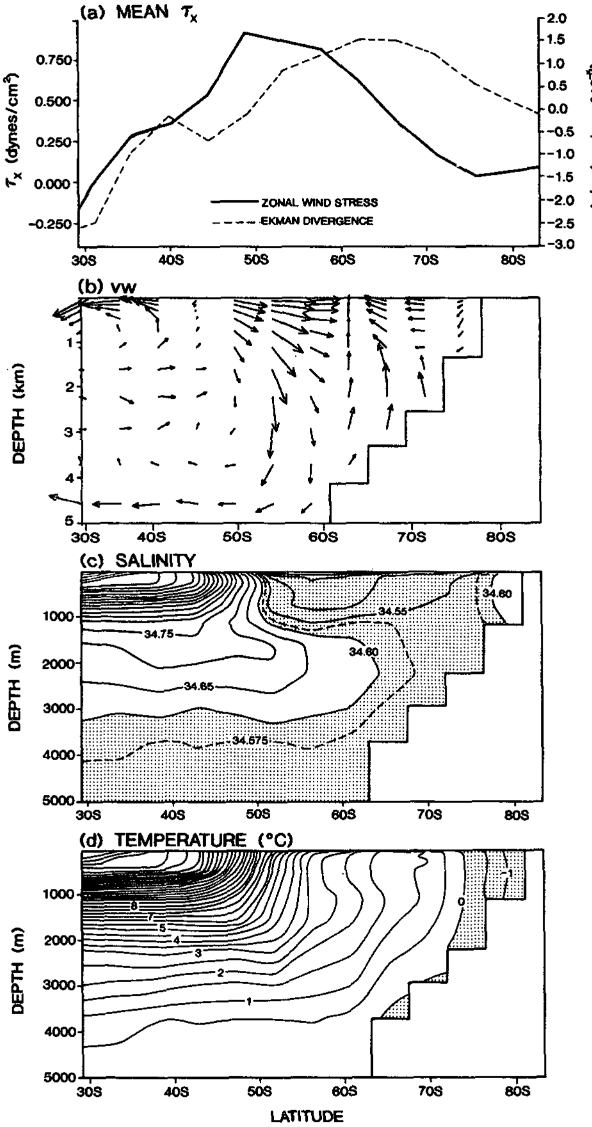

FIG. 14. Water masses and overturning in the 500-m restore model along a north–south transect terminating in the Ross Sea. Model properties are averaged over three grid rows centered on 174°W. Panel (a) shows the mean east–west component of the applied wind stress and the Ekman divergence (derived from the full wind stress field). Panel (b) shows the average v and w components of the model circulation plotted as current vectors. Current vectors for the surface layer are not included. Panels (c) and (d) show model salinity and temperature along the transect.

become bottom water with only minimal modifications. The most significant modifications occur on continental shelves where a fairly small volume of water is isolated from the deep water offshore and cooled to the freezing point over a period of several years.

7. Conclusions

Certain water masses on the continental shelves around Antarctica, the Weddell Sea's western shelf water, and the Ross Sea's high salinity shelf water are as much as 0.50 salinity units saltier than the water types from which they were formed. This salt enrichment is clearly due to sea ice brine. These high-salinity shelf waters seem to form in fairly small quantities and are never observed leaving the shelves in their pure form. They flow off the shelves and contribute to the formation of bottom water, only after being diluted with glacial meltwater or shelfedge water masses. This dilution reduces the salt enrichment in the offshelf flow to about 0.15–0.20 units. Thus, the formation of sea ice does not increase the salinity of new bottom water very much. The relatively high salinity of Antarctic Bottom Water is mainly due to the fact that 34.70 psu

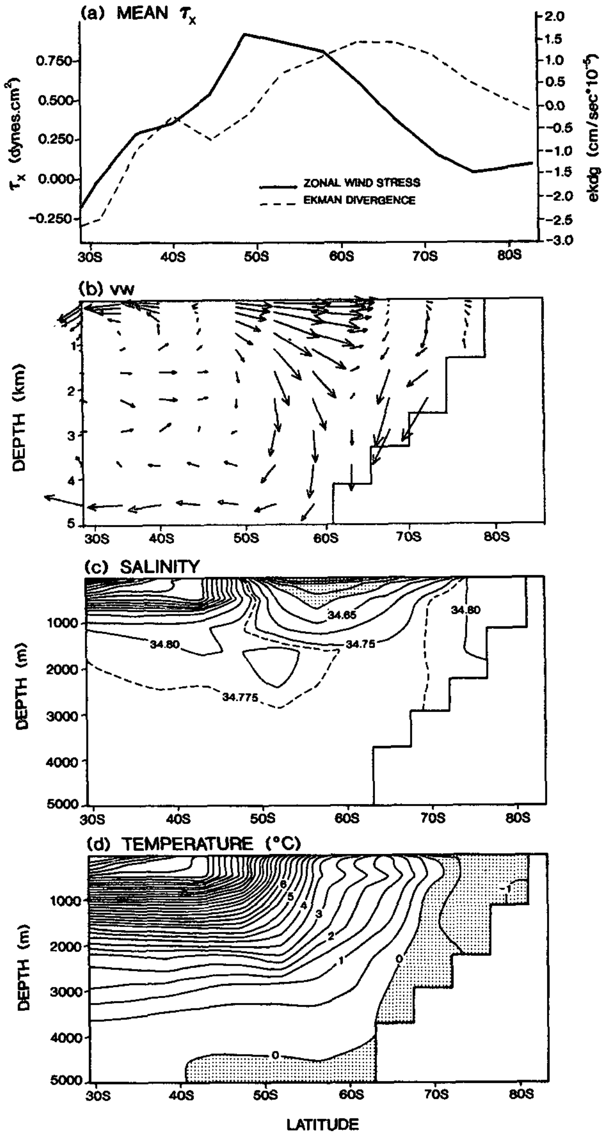

FIG. 15. Water masses and overturning along 174°W in the Antarctic Salt model. Panels (a)–(d) are described in caption to Fig. 14.

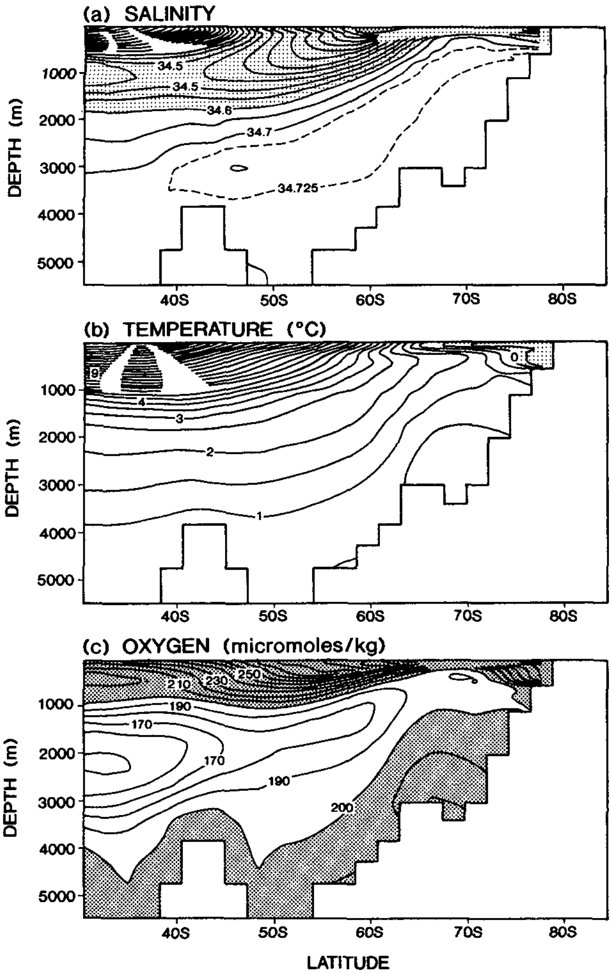

FIG. 16. Observed salinity, temperature, and oxygen along 174°W in the Ross Sea sector of the Southern Ocean. Observations from Levitus (1982) have been interpolated onto a two-degree grid.

Circumpolar Deep Water, and not 33.80 Antarctic surface water, dominates the mixture of water masses modified on the shelves (Jacobs et al. 1985). Were the mixture of water masses to somehow shift toward the fresh surface waters, the salt contributions from present sea ice production levels would be unable to maintain the salinity or density of new bottom water.

In this paper we have tried to determine the salt flux and the level of salinity enrichment appropriate for GCM boundary conditions in the vicinity of Antarctica. Jacobs et al. (1985) have determined that more than half the brine produced on the Ross Sea shelf negates local additions of fresh water from precipitation and melting glacier ice. Thus, only the brine from $\leqslant$0.50 m of new sea ice, out of a total of about one meter formed annually, actually serves to increase the salinity of the offshelf flow. Since GCM boundary conditions are concerned only with the net flux of salt or freshwater through each surface grid box, it is only this component of sea ice formation that needs to be included in GCM boundary conditions. Salt inputs of this magnitude have a very small effect on model salinities. If ocean GCMs predict interior salinities that are too fresh, modelers do not have the liberty of adjusting Antarctic boundary conditions to make model salinities substantially higher.

Model boundary conditions that produce large increases in Antarctic salinity, like those in our Antarctic Salt model, alter large volumes of near-surface water seaward of the continental shelves. Perhaps an order of magnitude more salt is added than can be justified by shelf water budgets. These large salt fluxes drive huge amounts of deep convection in a region where deep convection is rarely observed. They convert large quantities of near-surface water into new deep water. Application of this kind of boundary condition grossly mischaracterizes the processes of bottom-water formation around Antarctica.

Acknowledgments. We would like to thank Ron Stouffer, Keith Dixon, and Steve Carson for helpful internal reviews. Stan Jacobs, Hartmut Hellmer, and an unknown reviewer helped set us straight on our naive initial characterization of Antarctic shelf oceanography. Jeff Varanyak, Cathy Raphael, and Phil Tunison drafted the figures. Wendy Marshall prepared the tables.

REFERENCES

Brennecke, W., 1921: Die ozeanographischen Arbeiten der Deutsch Antarktischen Expedition 1911–1932. *Archiv. Deutschen Seewarte,* **39**(1), 214 pp.

Broecker, W. S., 1986: Oxygen isotope constraints on surface ocean temperature. *Quatern. Res.*, **26**, 121–134.

——, T. Takahahsi, and T. Takahashi, 1985: Sources and flow patterns of deep-ocean waters as deduced from potential temperature, salinity, and initial phosphate concentration. *J. Geophys. Res.*, **90**, 6925–6939.

Bryan, K., and L. J. Lewis, 1979: A water mass model of the World Ocean. *J. Geophys. Res.*, **84**, 2503–2517.

Cox, M. D., 1989: An idealized model of the world ocean. Part I: The global-scale water masses. *J. Phys. Oceanogr.*, **19**, 1730–1752.

Craig, H., and L. I. Gordon, 1965: *Deuterium and Oxygen-18 Variations in the Ocean and the Atmosphere.* Consiglio Nationalle delle Richerche Laboratorio de Geologia Nucleare, 122 pp.

Deacon, G. E. R., 1937: The hydrology of the Southern Ocean. *Discovery* Rep. 15, 1–124, plates I–XLIV.

England, M. H., 1992: On the formation of Antarctic Intermediate and Bottom Water in ocean general circulation models. *J. Phys. Oceanogr.*, **22**, 918–926.

——, 1993: On the formation of global-scale water masses in ocean general circulation models. *J. Phys. Oceanogr.*, **23**, 1523–1552.

Foldvik, A., T. Gammelsrod, and T. Torrensen, 1985: Circulation and water masses on the southern Weddell Sea Shelf. *Oceanology of the Antarctic Continental Shelf,* S. Jacobs, Ed., Antarctic Res. Ser., Vol. 43, Amer. Geophys. Union, 5–20.

Foster, T. D., and E. C. Carmack, 1976: Frontal zone mixing and Antarctic Bottom Water formation in the southern Weddell Sea. *Deep-Sea Res.*, **23**, 301–317.

Gill, A. E., 1973: Circulation and bottom water production in the Weddell Sea. *Deep-Sea Res.*, **20**, 111–140.

Gordon, A. L., 1981: Seasonality of Southern Ocean sea ice. *J. Geophys. Res.*, **86**, 4193–4197.

——, B. A. Huber, H. H. Hellmer, and A. Ffield, 1993: Deep and bottom water of the Weddell Sea's western rim. *Science,* **262,** 95–97.
Grootes, P. M., and M. Stuiver, 1983: Ross Ice Shelf oxygen isotope profile at J-9. *Antarct. J. U. S.,* **18,** 107–109.
Hellerman, S., and M. Rosenstein, 1983: Normal monthly wind stress over the world ocean with error estimates. *J. Phys. Oceanogr.,* **13,** 1093–1104.
Jacobs, S. S., A. L. Gordon, and J. L. Ardai, 1979: Circulation and melting beneath the Ross Ice Shelf. *Science,* **203,** 439–442.
——, R. G. Fairbanks, and Y. Horibe, 1985: Origin and evolution of water masses near the Antarctic continental margin: Evidence from $H_2{}^{18}O/H_2{}^{16}O$ ratios in seawater. *Oceanology of the Antarctic Continental Shelf,* Antarctic Res. Ser., Vol. 43, Amer. Geophys. Union, 59–85.
Killworth, P. D., 1977: Mixing on the Weddell Sea continental slope. *Deep-Sea Res.,* **24,** 427–448.
Levitus, S., 1982: *Climatological Atlas of the World Ocean.* NOAA Prof. Paper 13, U. S. Govt. Printing Office, Washington, DC, 173 pp.
Maier-Reimer, E., U. Mikolajewicz, and K. Hasselmann, 1993: Mean circulation of the Hamburg LSG OCGM and its sensitivity to the thermohaline surface forcing. *J. Phys. Oceanogr.,* **23,** 731–757.
Martinson, D. G., 1990: Evolution of the Southern Ocean winter mixed layer and sea ice: Open ocean deepwater formation and ventilation. *J. Geophys. Res.,* **95,** 11 641–11 654.
Mosby, H., 1934: *The Waters of the Atlantic Antarctic Ocean.* Jacob Dybwad, 131 pp.
Schlosser, P., R. Bayer, A. Foldvik, T. Gammelsrod, G. Rohardt, and K. O. Munnich, 1990: Oxygen 18 and helium as tracers of ice shelf water and water/ice interaction in the Weddell Sea. *J. Geophys. Res.,* **95,** 3253–3263.
——, J. L. Bullister, and R. Bayer, 1992: Studies of deep water formation and circulation in the Weddell Sea using natural and anthropogenic tracers. *Mar. Chem.,* **35,** 97–122.
Toggweiler, J. R., and B. Samuels, 1993: New radiocarbon constraints on the upwelling of abyssal water to the ocean's surface. *The Global Carbon Cycle,* M. Heimann, Ed., NATO ASI Series, Springer-Verlag, 333–366.
——, K. Dixon, and K. Bryan, 1989a: Simulations of radiocarbon in a coarse-resolution world ocean model, 1. Steady state prebomb distributions. *J. Geophys. Res.,* **94,** 8217–8242.
——, ——, and ——, 1989b: Simulations of radiocarbon in a coarse-resolution world ocean model, 2. Distributions of bomb-produced carbon 14. *J. Geophys. Res.,* **94,** 8243–8264.
Warren, B. A., 1981: Deep circulation of the World Ocean. *Evolution of Physical Oceanography. Scientific Surveys in Honor of Henry Stommel,* B. A. Warren and C. Wunsch, Eds., The MIT Press, 6–41.
Weiss, R., H. G. Ostlund, and H. Craig, 1979: Geochemical studies of the Weddell Sea. *Deep-Sea Res.,* **26A,** 1093–1120.